THE JOURNAL OF BIOLOGICAL CHEMISTRY VOL. 286, NO. 28, pp. 25134–25144, July 15, 2011

Chemical Modifications in Therapeutic Protein Aggregates Generated under Different Stress Conditions

Received for publication, July 1, 2010, and in revised form, April 10, 2011 Published, JBC Papers in Press, April 25, 2011, DOI 10.1074/jbc.M110.160440

Quanzhou Luo[‡1], **Marisa K. Joubert**[§], **Riki Stevenson**[§], **Randal R. Ketchem**[¶], **Linda O. Narhi**[§], **and Jette Wypych**[‡2]

From the Departments of [‡]*Analytical and Formulation Sciences and* [§]*Formulation and Analytical Resources, Amgen Inc., Thousand Oaks, California 91320 and the* [¶]*Department of Protein Science, Amgen Inc., Seattle, Washington 98119*

In this study, we characterized the chemical modifications in the monoclonal antibody (IgG_2) aggregates generated under various conditions, including mechanical, chemical, and thermal stress treatment, to provide insight into the mechanism of protein aggregation and the types of aggregate produced by the different stresses. In a separate study, additional biophysical characterization was performed to arrange these aggregates into a classification system (Joubert, M. K., Luo, Q., Nashed-Samuel, Y., Wypych, J., and Narhi, L. O. (2011) *J. Biol. Chem.* 286, 25118–25133). Here, we report that different aggregates possessed different types and levels of chemical modification. For chemically treated samples, metal-catalyzed oxidation using copper showed site-specific oxidation of Met^{246}, His^{304}, and His^{427} in the Fc portion of the antibody, which might be attributed to a putative copper-binding site. For the hydrogen peroxide-treated sample, in contrast, four solvent-exposed Met residues in the Fc portion were completely oxidized. Met and/or Trp oxidation was observed in the mechanically stressed samples, which is in agreement with the proposed model of protein interaction at the air-liquid interface. Heat treatment resulted in significant deamidation but almost no oxidation, which is consistent with thermally induced aggregates being generated by a different pathway, primarily by perturbing conformational stability. These results demonstrate that chemical modifications are present in protein aggregates; furthermore, the type, locations, and severity of the modifications depend on the specific conditions that generated the aggregates.

Immunoglobulin G (IgG) monoclonal antibodies represent a rapidly growing drug class in the biopharmaceutical industry for the treatment and prevention of disease (1–3). Although antibodies are relatively stable, they can undergo a variety of degradations during manufacturing, formulation, and storage. Protein aggregates, one of the most common degradants in the preparation of high concentration protein therapeutics, have been proposed to cause adverse effects, such as reduced efficacy and immunological reactions (4–7), although direct evidence supporting these effects in humans is not currently available. It is therefore very important to characterize the biophysical and biochemical properties of aggregates to better assess their safety and efficacy. It is also very important to understand the underlying mechanisms of protein aggregation, which requires thorough characterization of different aggregate species.

Chemical modifications may play a role in protein aggregation (8), which includes reactions such as isomerization, deamidation, oxidation, and peptide bond cleavage (8, 9). Deamidation can cause structurally and biologically important alterations in peptides and proteins through the introduction of unfavorable negative charge (10–14). The susceptibility of a specific Asn to deamidation is a function of neighboring amino acids, tertiary structure, and solution conditions, including pH, temperature, and ionic strength (11, 12). The primary sequence is one of the main contributions to deamidation rates with the amino acid residues adjacent to Asn being especially significant. Gly in the C-terminal position in model proteins has been found to result in the most deamidation of Asn (10).

Oxidation is one of the major degradation pathways for protein therapeutics under stress conditions (15–18). Cys, Met, Trp, and His are all prone to oxidation. The thiol group in the exposed Cys residues is a highly reactive functional group (19). Oxidation reactions can be promoted by light exposure, transition metals, peroxide from or induced by excipients, or simply the presence of oxygen during the manufacturing and storage process (20–23). Metal-catalyzed oxidation occurs in the presence of oxygen, transition metals (iron and copper, in particular) (24), and a reducing agent that can convert oxygen to a reactive oxygen species (O_2^- or $OH^\bullet$) and the transition metal to its reduced form (25). A unique feature observed during the metal-catalyzed oxidation of proteins is that only a few amino acid residues located in close proximity to each other are modified (25–27). This site specificity is dependent on the metal-binding site where the reactive oxygen species are generated and also the half-life of reactive oxygen species. The reactive oxygen species are hindered from diffusing into the surrounding medium because they react quickly with amino acid residues near the site of generation (26, 27).

In a separate study (28), we applied various stress conditions to generate different populations of IgG2 aggregates. These stresses varied from very mild to harsh and were chosen as accelerated conditions based on the types of stress that might be encountered during the manufacturing process and to result in a wide range of different aggregate populations. The stress conditions used to generate IgG2 aggregates can also induce chemical modifications in proteins, and indeed, chemical modification could contribute to aggregation of the protein. Therefore, it is essential to determine whether chemical modifications are present in these different aggregate types, which can provide clues as to the underlying mechanism of aggregate for-

[1] To whom correspondence may be addressed. Tel.: 805-447-6034; Fax: 805-376-2354; E-mail: qluo@amgen.com.
[2] To whom correspondence may be addressed. Tel.: 805-447-4207; Fax: 805-375-3378; E-mail: jwypych@amgen.com.

mation and the potential impact of chemical modifications on specific characteristics of the aggregates. In this study, we use LC-MS/MS to characterize the chemical modifications of the aggregates of an IgG_2 formed under different conditions, including mechanical, chemical, and thermal stress treatment.

EXPERIMENTAL PROCEDURES

Materials—The recombinant IgG2 monoclonal antibody (mAb1) used in this study was produced at Amgen Inc. (Thousand Oaks, CA) and consisted of two human γ HCs and two human κ LCs. The antibody was expressed in Chinese hamster ovary cells and highly purified using well established chromatographic procedures developed at Amgen (29). The T_m of the mAb1 was assessed using differential scanning calorimetry, and the sample in 10 mM sodium acetate, pH 5, showed a T_m at ~74.2 °C. Trypsin and endoproteinase Glu-C (Glu-C) were obtained from Roche Diagnostics. Guanidine hydrochloride (GdnHCl) and urea were obtained from ICN Biomedicals Inc. (Aurora, OH). Dithiothreitol, iodoacetic acid sodium salt, ascorbic acid, EDTA, and Tris base were obtained from Sigma. Trifluoroacetic acid (TFA) was from Pierce. NAP™-5 columns were from GE Healthcare.

Aggregate Preparation and Biophysical Characterization—As described in the accompanying article (28), mAb1 aggregates were generated under various conditions. Briefly, for syringe stress, the protein samples were pumped 50 times through a disposable 18-gauge × 1.5-inch needle (VWR Scientific) attached to either a 3-ml disposable syringe containing silicone oil (Fisher) (syringe-so$^+$), or through a Daikyo Crystal Zenith syringe that is silicone oil-free (West Pharmaceutical Services) (syringe-so$^-$). For stirring stress, 2 ml of the protein sample was stirred with a 6 × 6-mm Teflon stir bar at ~700 rpm in a glass vial capped and placed vertically on a magnetic stir plate over 20 h (stir-20h) or for 3 days (stir-3d). For thermal stress, the protein solution (1 mg/ml) was either incubated at 90 °C overnight (90C) or diluted to 1 mg/ml in 10 mM acetate, pH 8.5, followed by incubation at 65 °C for 1 h (65C/pH 8.5). For hydrogen peroxide oxidation, 0.1% H_2O_2 was added to the protein, and the solution was incubated for 20 h at 37 °C and quenched with 80 mM Met aqueous solution. For metal-catalyzed oxidation, protein solution (1 mg/ml) was oxidized with 5 mM $CuSO_4$ and 4 mM ascorbic acid overnight at 37 °C and then the reaction was quenched with 5 mM EDTA. After quenching, H_2O_2 and metal samples were dialyzed overnight into 10 mM acetate, pH 5.0. To compare the chemical modifications in supernatant and pellet fractions, the total stressed samples were centrifuged at 12,000 rpm for 5 min, and the supernatant and pellet were separated by carefully removing the supernatant using a pipette.

Size-exclusion-High Performance Liquid Chromatography (SE-HPLC)—The supernatant fractions of the stressed samples were subjected to SE-HPLC analysis. An Agilent 1100 HPLC system with a binary pump was equipped with a UV detector and an autosampler. The proteins were injected onto a Tosoh Bioscience TSK-Gel G3000SWxl column (7.8 × 300 mm, 5-μm particles) operated at room temperature. The flow rate was 0.5 ml/min, and the eluted proteins were monitored by UV absorption (280 nm wavelength). The mobile phase contained 100 mM sodium phosphate, 250 mM sodium chloride, pH 6.8.

Enzyme Digestion of Stressed Samples—mAb1 total stressed samples and their supernatant and pellet fractions were dissolved in GdnHCl and 0.1 M Tris buffer to achieve a final concentration of 6.5 M GdnHCl. Reduction was conducted with 10 mM dithiothreitol (final concentration), followed by alkylation with 20 mM iodoacetamide for 15 min in the dark at room temperature. NAP™-5 columns were then used to exchange the reduced and alkylated samples into 50 mM Tris buffer, pH 7.5. The proteolytic enzyme (trypsin or Glu-C) was added to the samples of the reduced and alkylated protein to achieve a protein:enzyme ratio of ~20:1 (w/w) and incubated at 37 °C overnight. Met was added (~12 mM final concentration) to the sample to inhibit method-induced oxidation. The mixture was acidified with 5% TFA to quench the digestion. Two complementary peptide maps, generated by trypsin and Glu-C, were performed to characterize the chemical modifications in the stressed samples. The trypsin peptide map was employed as the primary map. A complementary Glu-C peptide map was performed to obtain full sequence coverage.

LC/ESI-MS/MS Analysis—The on-line LC/ESI-MS/MS[3] analyses were performed using an Agilent 1200 HPLC system directly coupled with a Thermo Scientific (San Jose, CA) LTQ XL ion trap mass spectrometer equipped with an electrospray ionization source. The antibody digests were separated using a RP-HPLC column (Phenomenex Jupiter C5, 2 × 250 mm, 300-Å pore size, 5-μm particle size), with the column temperature maintained at 50 °C. The mobile phase A was 0.1% (v/v) TFA in water, and the mobile phase B was 0.1% TFA and 90% acetonitrile in water. A gradient (hold at 2% B for 5 min, 2–22% B for 25 min, and then 22–42% B within 95 min) was used to separate the digested peptides at a flow rate of 0.2 ml/min. The eluted peptides were monitored by both UV absorption (214 nm wavelength) and mass spectrometry. The solvent peaks were diverted to the waste before the flow entered the ESI source. The ESI source voltage of the LTQ was set at 4.5 kV and the capillary temperature at 275 °C. For MS experiments, mass spectra were acquired from 300 to 2000 m/z in the positive mode, followed by a data-dependent ultra zoom scan to determine the charge state of the most intense ion and a MS/MS scan to identify the sequence of the peptide precursor ion. In the MS/MS scan, the precursor ions were fragmented by collision-induced dissociation (CID) with 35% relative collision energy. Peptides were identified using Mass Analyzer (30), an in-house developed software, which correlates the experimental tandem mass spectra against the theoretical tandem mass spectra generated of known peptide sequences. The quantitative results of chemical modifications on an amino acid can be determined by comparing the selected-ion chromatogram (SIC) of the parent

[3] The abbreviations used are: LC/ESI-MS, liquid chromatography electrospray ionization mass spectrometry; LC, light chain; HC, heavy chain; RP-HPLC, reversed-phase HPLC; Glu-C, endoproteinase Glu-C; H_2O_2, hydrogen peroxide; SIC, selected ion chromatogram; CDR, complementarity determining region; PDB, Protein Data Bank; GdnHCl, guanidine hydrochloride; SO, silicone oil; SAS, solvent-accessible surface area; CID, collision induced dissociation; SE-HPLC, size-exclusion-HPLC.

TABLE 1
The analyzed mAb1 aggregates stressed under different conditions

Stress treatment[a]
Mechanical stress
Syringe-so$^-$
Syringe-so$^+$
Stir-20h
Stir-3d
Chemical treatment
Metal
H_2O_2
Thermal stress
65 °C/pH 8.5
90 °C

[a] For detailed stress conditions see our accompanying article (28).

peptides and their modified counterparts using Qual Browser of Xcalibur software from Thermo Scientific.

Molecular Modeling—A molecular model was generated of the mAb1 variable domain, combining framework and complementarity determining region (CDR) structures from the Protein Data Bank (PDB) using Molecular Operating Environment (MOE) software (Chemical Computing Group, Montreal, Quebec, Canada). The Antibody Modeler component of the MOE software was used to build the model. The framework structure was chosen from the PDB based on percent of amino acid identity and conservation, a structure rating factor, and the combination of the light chain variable domain and heavy chain variable domain scores. CDR structures were first limited by length and then chosen based on percent identity and conservation, with structural outliers being removed. The final model was structurally refined and energy-minimized with MMFF94 force field parameters and checked for allowed Ramachandran ϕ-ψ angles, bond angles and lengths, and conserved positive ϕ angles (31–33). Solvent accessibility calculations were performed by MOE software, using a 1.4-Å solvent radius consistent with H_2O, on the homology-derived computational molecular model for the variable domain, PDB code 2QSC for constant region one of the heavy chain domain, and PDB code 1T89 for the Fc region. The theoretical maximum solvent accessibility was calculated on the Gly-Xaa-Xaa-Xaa-Gly sequence, where Xaa-Xaa-Xaa is the residue of interest, extracting the three residues and their actual dihedral angles. The percentage of solvent accessibility was calculated by dividing the actual solvent accessibility in the context of the entire structure by the theoretical maximum in its particular environment. Individual models and structures for separate domains were chosen based on sequence homology for the most accurate data. Full-length human antibody IgG_1 b12, PDB entry 1HZH (34), was utilized to create the full-length figure and zoomed image of the Fc region.

RESULTS

As described in the accompanying article (28), various stress conditions were used to generate aggregates of mAb1. Table 1 shows how sample treatment results in different aggregates, which were thoroughly biochemically characterized in this study. The supernatant fractions of the stressed samples were evaluated by SE-HPLC to quantify the amount of monomer, oligomers, and fragments. A TSK-Gel G3000SWxl column, which provides a calibration range of 10,000–500,000 for globular proteins, was used for the analysis such that oligomers and fragments can be clearly resolved from the monomers. Oligomers were detected in the stir-20h (11.1 ± 0.7%) and 65C/pH 8.5 (3.3 ± 0.4%) samples. Fragments were only detected in the 65C/pH 8.5 (1.1 ± 0.3%) and 90C (100.0 ± 0.0%) samples, indicating that peptide bond cleavage occurred under the chosen thermal stress conditions. For untreated, syringe-so$^-$, syringe-so$^+$, and H_2O_2-treated samples, very low amounts of oligomers (0.4 ± 0.1%), but no fragments, were detected. The stir-3d sample was not characterized because the amounts of protein remaining in the supernatant fraction were below the detection limit of SE-HPLC. Because of the interference of the UV absorbance of copper, the supernatant fraction of the metal-stressed sample was not analyzed by SE-HPLC.

Characterization of the Mechanically Stressed Samples—In this study, we focused on the syringe- and stirring-stressed samples as those mimic the "real life" mechanical stresses that biopharmaceuticals may experience during manufacturing and injection. No oxidation of Cys residues was detected in this study, indicating that the intramolecule disulfide bonds might be completely formed and not affected by the stress treatments used in this study.

mAb1 contains six Met, nine Trp, and eight His residues on each of the heavy chains and three Trp and three His residues on each of the light chains. Among them, one Met (Met^{34} in the Fab of the heavy chain), two Trp (Trp^{104} in the Fab of the heavy chain and Trp^{98} in the Fab of the light chain), and one His (His^{94} in the Fab of the light chain) are located in the CDR of mAb1, as highlighted in Fig. 1. The locations of all the Met (*red*), Trp (*blue*), and His (*charcoal*) residues of the mAb1 as well as their corresponding tryptic peptides containing the labile amino acids are shown in Fig. 1. Oxidation at Met, Trp, and His sites was characterized through peptide mapping. The diluted samples before stress treatment were used as negative controls. Chemical modifications in the total stressed samples as well as the supernatant and pellet fractions were calculated by comparing the peak area under the SIC of the modified and unmodified peptides in a single LC/MS analysis. Thus, the protein concentration in pellet and supernatant should not affect the results. As an example, six Met-containing peptides, H3 (Met^{34}), H9 (Met^{82}), H20 (Met^{246}), H32–33 (Met^{352}), H36 (Met^{391}), and H39 (Met^{422}) were identified by MS/MS in the peptide map of the negative control sample (*top panel* in Fig. 2), and no modified forms of the peptides were detected. The fact that no oxidation was detected in the control suggests that the analytical process does not create oxidation artifacts. In the sample that was stirred for 20 h, six new peptides with a mass increase of 16 Da were observed in the peptide map of the total stressed sample. The MS/MS analysis revealed that the +16-Da species are the oxidized forms, with Met being oxidized to the sulfoxide form (*bottom trace* in Fig. 2). Oxidized Met is more polar and less hydrophobic, which leads to decreased retention relative to the corresponding parent peptides on the RP-HPLC column. For certain peptides containing Met residues, the oxidized products resolved sufficiently from the parent counterparts and other unrelated peptides such that the UV signal could be used to quantify the levels of oxidation. Fig. 3 shows a region of the peptide map of the total unfractionated stir-20h sample and

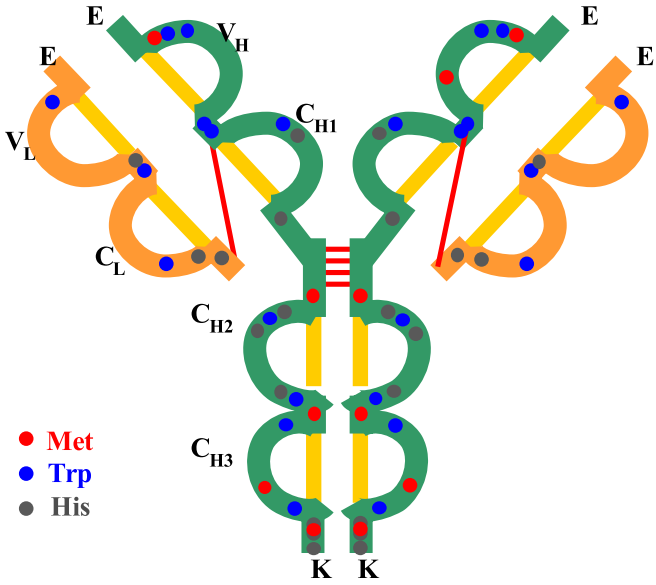

	AA	Tryptic Peptide	AA	Tryptic Peptide	AA	Tryptic Peptide
HC	Met^{34}	H3	Trp^{36}	H3	His^{166}	H15
	Met^{82}	H9	Trp^{47}	H5	His^{202}	H15
	Met^{246}	H20	Trp^{104}	H12	His^{262}	H21
	Met^{352}	H32-33	Trp^{105}	H12	His^{279}	H21
	Met^{391}	H36	Trp^{156}	H15	His^{304}	H24
	Met^{422}	H39	Trp^{271}	H21	His^{423}	H39
			Trp^{307}	H24	His^{427}	H39
			Trp^{375}	H35	His^{429}	H39
			Trp^{411}	H39		
LC			Trp^{36}	L3	His^{94}	L7
			Trp^{98}	L7	His^{191}	L17
			Trp^{150}	L13	His^{200}	L18

FIGURE 1. **Schematic diagrams of mAb1 showing the distribution of Met/Trp/His and the corresponding tryptic peptides containing the labile amino acids.** Met residues are represented in *red*, Trp residues in *blue*, and His in *charcoal*. The highlighted Met^{34} (HC), Trp^{104} (HC), Trp^{98}(LC), and His^{94} (LC) are in the CDR of the mAb1.

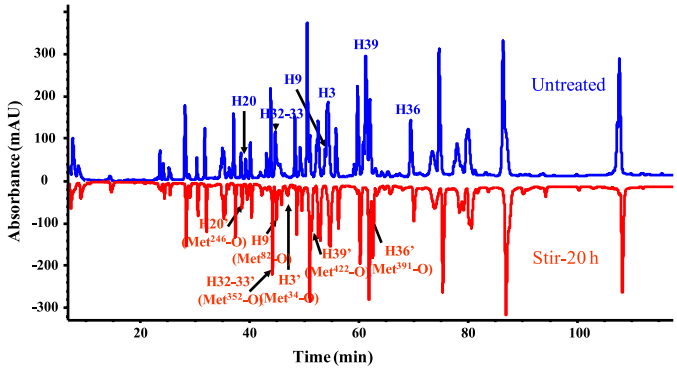

FIGURE 2. **Trypsin peptide maps of untreated and mechanically stressed mAb1 by mild stirring (stir-20h).** *Top trace* in *blue* is untreated mAb1. The six peaks (H3, H9, H20, H32–33, H36, and H39) corresponding to tryptic peptides containing Met residues are labeled. *Bottom trace* in *red* is the stir-20h mAb1. The six peaks (H3′, H9′, H20′, H32–33′, H36′, and H39′) corresponding to oxidized Met-containing peptides are labeled. *mAU*, milli-absorbance units.

focuses on the profile changes occurring for the Met^{34}-containing peptide H3. UV and SIC traces are provided for comparison. Met^{34} was oxidized at 12.5% as measured using UV integration, which is consistent with the value (11.4%) obtained by using the SIC approach. Because the SIC approach was in good agreement with the UV-based quantitation (14), it was used to quantify chemical modifications at all labile amino acid residues, which allowed quantitation of modifications that were not sufficiently resolved from other peptides in the UV chromatogram or for which the modification level was too low to be quantified by UV. The modifications in the total stressed samples as well as the supernatant and pellet fractions were calculated by comparing the peak area under the SIC of the modified and unmodified peptides in a single LC/MS analysis. Thus, the protein concentration in pellet and supernatant should not affect the results.

Table 2 summarizes the oxidation level of Met and Trp residues in the untreated and mechanically stressed mAb1 samples as well as the calculated solvent-accessible surface areas (SAS) of the amino acids. Human IgG_1 and IgG_2 sequences are highly conserved in the Fc domain, with ~94% sequence identity. Because the overall tertiary fold in this region is likely to be very similar as well, the human IgG_1 Fc structure could serve as a reasonable surrogate for the human IgG_2 Fc structure. The calculated solvent accessibility reflects the percent of the residue that is on the surface of the folded protein based on the molecular model. Residues that are more surface-exposed are expected to be more available for oxidation and other chemical modifications. The SAS of the Met residues in the IgG_2 Fc portion, Met^{246}, Met^{352}, and Met^{422}, were calculated from the crystal structure of the IgG_1 Fc, and the levels are 30, 33, and 7%, respectively. Met^{391}, which is also in the Fc portion of IgG_2, corresponds to Val^{397} in the IgG_1 structure, and the SAS level of Val^{397} in the IgG_1 structure is 19%. The SAS of the two Met residues in the IgG_2 Fab portion, Met^{34} and Met^{82}, are calculated based on the homology model built on structures in the PDB, and they are completely buried in the molecule. The SAS of the Trp residues are calculated in the same way, and all five modified out of a total of twelve Trp residues show low solvent accessibility (1–8%).

For syringe-stressed samples, only Met oxidation was observed at several residues. Higher levels of Met oxidation were observed in the pellet fractions than in the supernatant and the total stressed samples. As an example, five Met residues, Met^{34}, Met^{82}, Met^{246}, Met^{391}, and Met^{422}, were oxidized in the pellet fraction of the sample stressed by being passed through a syringe in the presence of silicone oil (oxidation level varied from 4 to 18%), whereas only Met^{246} oxidation (5%) was observed in the total stressed sample, and no Met residues were oxidized in the protein from the supernatant fraction. In addition, no significantly different modifications between the two syringe-stressed samples were observed. Two different kinds of syringes, disposable polyethylene syringes containing silicone oil and silicone oil-free Daikyo Crystal Zenith cyclic polyolefin syringes, were used to generate aggregates, and the protein

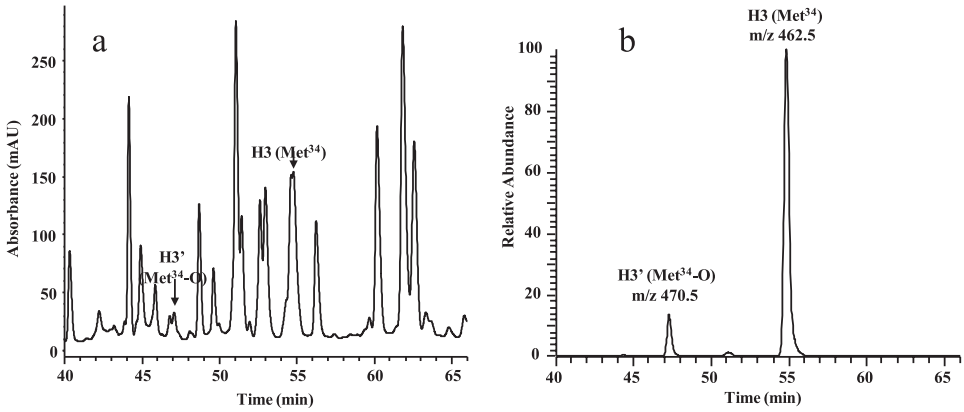

FIGURE 3. **Comparison of an oxidized peptide by UV light and MS.** A region of the trypsin peptide map showing the Met^{34}-containing peptide for mAb1 treated by mild mechanical stress (stir-20h) is depicted. *a,* UV profile at 214 nm. Milli-absorbance units (*mAU*). *b,* MS profile using SIC.

TABLE 2
Met and Trp oxidation (%) in mechanically stressed mAb1 samples

		Syringe-so$^+$			Syringe-so$^-$			Stir-20h			Stir-3d			
	Untreated	Total	Pellet	Supernatant	Total	Pellet	Supernatant	Total	Pellet	Supernatant	Total	Pellet	Supernatant	SAS[a]
														%
Met^{34} (HC)[b]	–[c]	–	17.1	–	–	9.1	–	11.4	12.7	10.5	41.0	35.5	40.3	<0.1
Met^{82} (HC)	–	–	18.0	–	–	–	–	15.0	11.4	12.2	36.4	37.7	33.4	<0.1
Met^{246} (HC)	–	4.9	12.1	–	4.4	11.2	4.0	17.2	15.5	15.5	51.5	45.6	47.9	30
Met^{352} (HC)	–	–	–	–	–	–	–	9.5	12.7	9.8	26.5	33.4	36.3	33
Met^{391} (HC)	–	–	7.2	–	–	–	–	10.3	9.9	10.0	43.9	40.4	40.3	19[d]
Met^{422} (HC)	–	–	3.5	–	–	3.7	–	8.9	10.3	8.9	34.3	31.2	32.7	7
Trp^{36} (LC)[e]	–	–	–	–	–	–	–	–	1.3	–	4.2	4.8	4.2	1
Trp^{47} (HC)	–	–	–	–	–	–	–	–	2.5	–	2.8	10.3	3.9	8
Trp^{156} (HC)	–	–	–	–	–	–	–	1.3	1.2	–	6.6	5.5	5.6	2
Trp^{98} (LC)	–	–	–	–	–	–	–	2.3	3.7	–	7.9	13.0	7.3	5
Trp^{271} (HC)	–	–	–	–	–	–	–	–	2.3	–	–	6.5	5.1	3

[a] SAS is of the modified amino acid residue.
[b] HC means heavy chain.
[c] – means not detected.
[d] SAS of Met^{391} is calculated from the crystal structure of PDB 1T89, and the value is the SAS of Val^{397}.
[e] LC means light chain.

solution was pumped through the syringes manually. As described in the accompanying article (28), these two different syringes were chosen to examine both the effect of syringe stress and the effect of silicone oil on the sample. The disposable polyethylene syringe is commonly used for injections of medication in the clinic, and the Daiyko syringe is made of material that is also commonly used to store and deliver medication in our company. Therefore, the small differences in modifications between the two populations of aggregates might be due to the slight differences in the strength of the stress used, the presence of silicone oil, the differences in the syringe material, leaching of metal ions from the needles, the air-liquid interface, or a combination of all.

In the peptide maps of the sample stirred for 20 h, a higher level of oxidation was observed at all six Met residues (oxidation level varied from 10 to 17%) along with a low level of oxidation (<4%) at five out of twelve Trp residues. The highest level of oxidation at the Met (oxidation level varied from 27 to 52%) and Trp (oxidation level varied from 3 to 13%) residues was observed in the stir-3d sample, indicating that Met is the most susceptible amino acid with respect to oxidation, whereas other amino acids require more stringent conditions to become oxidized. Thus, not surprisingly, more oxidation occurred when the protein was subjected to more severe mechanical stress.

TABLE 3
Met/Trp/His oxidation (%) in chemically modified mAb1 samples

		Metal				
	Untreated	Total	Pellet	Supernatant	H_2O_2, total	SAS[a]
						%
Met^{34} (HC)[b]	–[c]	5.5	6.6	5.1	9	<0.1
Met^{82} (HC)	–	6.0	5.1	4.7	–	<0.1
Met^{246} (HC)	–	22.8	22.2	22.3	100	30
Met^{352} (HC)	–	13.1	14.8	12.8	100	33
Met^{391} (HC)	–	12.5	14.3	12.0	100	19[d]
Met^{422} (HC)	–	11.1	10.3	12.1	100	7
Trp^{156} (HC)	–	22.8	20.1	18.9	–	2
His^{304} (HC)	–	1.4	2.8	1.6	–	18
His^{427} (HC)	–	10.7	10.1	8.5	–	86

[a] SAS is of the modified amino acid residue.
[b] HC means heavy chain.
[c] – means not detected.
[d] SAS of Met^{391} is calculated from the crystal structure of PDB 1T89, and the value is the SAS of Val^{397}.

Characterization of the Chemically Treated Samples—Table 3 lists the oxidation of Met, Trp, and His in the metal- and H_2O_2-treated mAb1 samples as well as their SAS. In addition to the oxidation of Met and Trp residues, we have detected oxidative damage of His residues. The two oxidized out of eleven His residues have quite different solvent accessibility, with the levels at 18 and 86% for His^{304} and His^{427}, respectively. His oxidation is not typically seen in aggregate from antibodies,[4] and

[4] Pavel Bondarenko, personal communication.

these aggregates also have copper still associated with the protein. This suggests that this type of aggregate would not be encountered under normal manufacturing or storage conditions. For the hydrogen peroxide-treated sample, four solvent-exposed Met residues in the Fc portion were completely oxidized. These residues are solvent-exposed and have been found in mAb and mAb aggregates previously (16, 35). In contrast, Met^{34} in the CDR region was partially oxidized (9%), and Met^{82} in the Fab of HC, which is not solvent-exposed, was not oxidized at all. Chemical modifications other than Met oxidation were not observed in H_2O_2-stressed samples. The chemical modifications of the supernatant and pellet fractions of the H_2O_2-stressed sample were not characterized because there was so little aggregate generated that it could not be isolated; thus, only the entire sample was analyzed.

For the metal-treated sample, the same levels of oxidation of Met, Trp, and His were observed in the supernatant fraction, pellet fraction, and total stressed sample. His has been identified as one amino acid particularly susceptible to metal-catalyzed oxidation (18, 36). Among the eleven His residues in this molecule, only His^{304} (~3%) and His^{427} (~11%) in the heavy chain were oxidized. Ultra zoom scan acquisition and CID MS/MS were performed on the His^{304}-containing peptide and its oxidized form. Based on the monoisotopic peaks obtained, a mass difference of +8 Da was observed for the doubly charged peak of the parent and oxidized species, indicating a +16-Da increase in the modified peptide (Fig. 4, *a* and *b*). Additional analysis, in which the doubly charged ions of the peptides were selected for CID MS/MS analysis and the MS/MS spectra of the parent and oxidized peptides were compared, demonstrated that the residue that has been modified can be easily distinguished by comparing the dissociation patterns of the oxidized and parent peptides. The majority of the product ions has been identified, and their assignments are labeled (Fig. 4, *c* and *d*). Both b and y fragment ion series were readily observed. The MS/MS spectrum of the oxidized peptide shows that b and y ions increase by 16 Da from b9 and y8, respectively, which unambiguously identified His^{304} as the oxidation site. A significant level of Trp^{156} oxidation (~23%) was also observed, and all six Met residues in the mAb1 molecule were oxidized, whereas the solvent-exposed Met residues showed a higher level of oxidation, and the highest level of oxidation was observed at Met^{246} (>23%).

Characterization of the Thermally Stressed Samples—Two conditions were used to generate the thermally stressed mAb1 aggregates as follows: incubation at 90 °C (90C) and a combination of treatment at 65 °C and basic pH (65C/pH 8.5). In these cases, observed modifications were Asn deamidation. Table 4 lists the Asn deamidation in the thermally stressed samples as well as their SAS. Deamidation is a common post-translational modification resulting in the conversion of an Asn residue to a mixture of isoaspartate and aspartate (10, 11). mAb1 presented in this study has nineteen Asn residues on each of the heavy chains and six on each of the light chains (Fig. 5). The solvent accessibility of the Asn residues varied widely from 4 to 82%. Asn^{309} and Asn^{378} in the Fc region are highly solvent-exposed with SAS levels of 64 and 82%, respectively. In addition, Asn^{309} and Asn^{378} are the only two Asn-Gly (NG) sites in the Fc por-

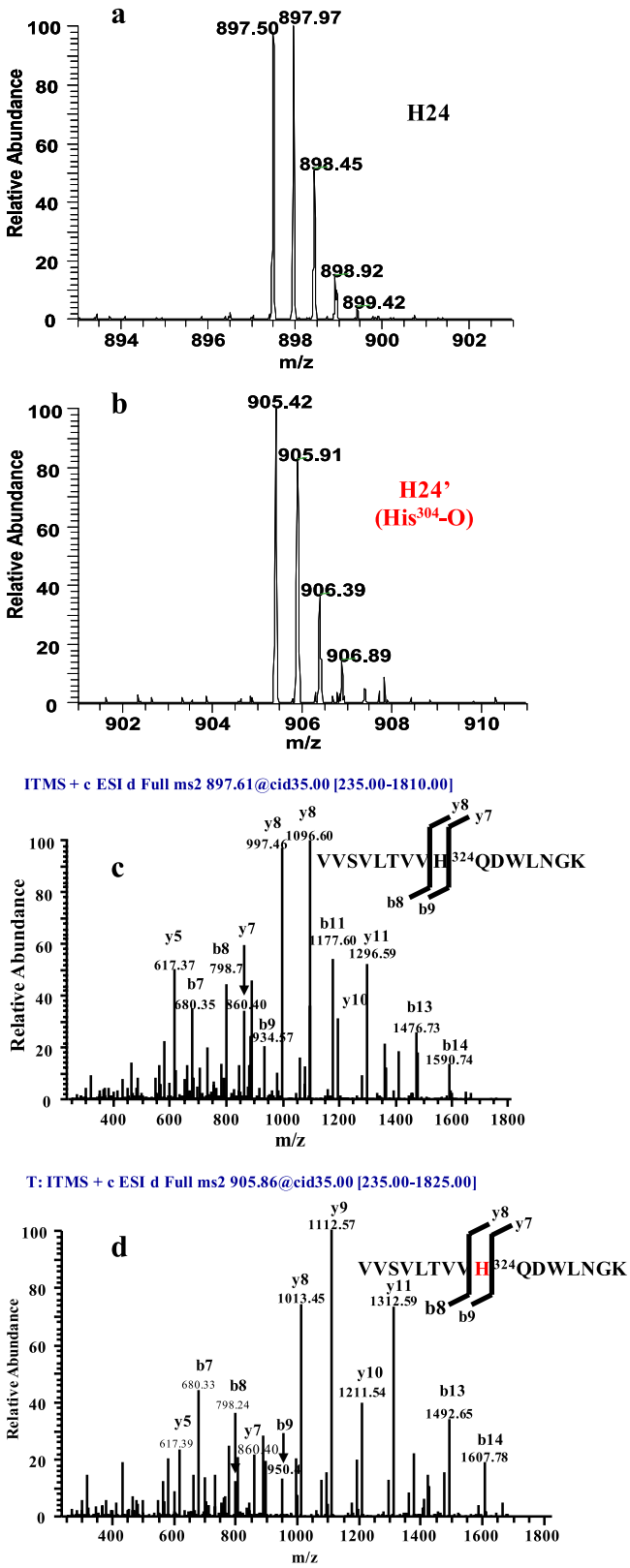

FIGURE 4. **MS spectral analysis of His^{304}- and oxidized His^{304}-containing peptides.** Ultra zoom scans for the doubly charged His^{304}- and oxidized His^{304}-containing peptides are shown in the untreated (*a*) and metal-treated (*b*) mAb1 samples, respectively. MS/MS spectra are shown of the His^{304}- (*c*) and oxidized His^{304} (*d*)-containing peptides and peak assignments for the production ion.

TABLE 4
Met oxidation and Asn deamidation (%) in thermally stressed mAb1 samples

		65C/pH 8			90C			
	Untreated	Total	Pellet	Supernatant	Mix	Pellet	Supernatant	SAS[a]
								%
Met[34] (HC)[b]	–[c]	–	–	–	3.8	4.3	5.3	<0.1
Met[246] (HC)	–	–	2.9	–	6.3	6.5	6.7	30
Met[422] (HC)	–	–	1.4	–	–	–	–	7
Asn[32] (HC)	–	–	–	–	50.0	48.5	49.5	14
Asn[73] (HC)	–	–	–	–	61.1	60.6	- -[d]	31
Asn[83] (HC)	–	–	–	–	43.7	38.6	- -	40
Asn[270] (HC)	–	–	–	–	20.2	20.1	- -	11
Asn[280] (HC)	–	–	–	–	31.9	30.6	30.4	63
Asn[309] (HC)	–	15.5	21.1	5.9	81.8	81.4	100	64
Asn[319] (HC)	–	–	–	–	90.3	87.9	100	9
Asn[355] (HC)	–	–	–	–	14.1	12.1	- -	63
Asn[378] (HC)	–	10.3	18.3	–	49.7	45.3	- -	82
Asn[428] (HC)	–				93.8	97.8	100	72
Asn[31] (LC)[e]	–	–	–	–	51.8	52.9	48.7	66
Asn[139] (LC)	–	–	–	–	44.7	55.6	- -	4
Asn[140] (LC)	–	–	–	–	18.4	23.2	- -	31
Asn[154] (LC)	–	–	–	–	61.9	64.7	- -	73
Asn[160] (LC)	–	–	–	–	6.3	7.4	8.1	28
Asn[212] (LC)	–	–	–	–	10.3	16.4	17.8	57

[a] SAS is of the modified amino acid residue.
[b] HC means heavy chain.
[c] – means not detected.
[d] Asn residues were not detected due to the peptide bond cleavage.
[e] LC means light chain.

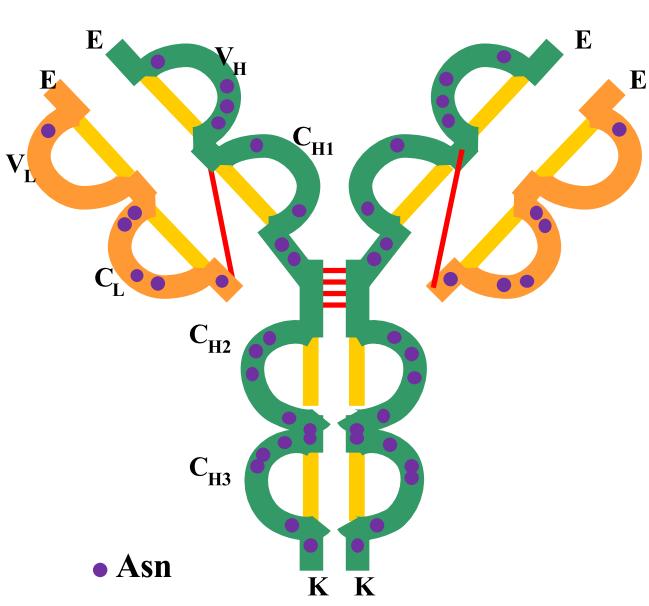

HC				LC	
AA	Tryptic Peptide	AA	Tryptic Peptide	AA	Tryptic Peptide
Asn[32]	H3	Asn[291]	H23	Asn[31]	L3
Asn[73]	H8	Asn[309]	H24	Asn[139]	L11
Asn[76]	H9	Asn[319]	H27	Asn[140]	L11
Asn[83]	H9	Asn[355]	H34	Asn[154]	L14
Asn[157]	H15	Asn[378]	H35	Asn[160]	L14
Asn[190]	H15	Asn[383]	H35	Asn[212]	L19
Asn[199]	H15	Asn[384]	H35		
Asn[206]	H15	Asn[415]	H39		
Asn[270]	H21	Asn[428]	H39		
Asn[280]	H21				

FIGURE 5. **Schematic diagrams of mAb1 showing the distribution of Asn and the corresponding tryptic peptides containing the labile amino acids.** Asn residues are represented in *brown*. The highlighted Asn[32] (HC) and Asn[31] (LC) are in the CDR of the mAb1.

tion of the molecule. For the 65 °C at pH 8.5 degraded sample, only one Asn residue (Asn[309]) was deamidated (~6%) in the supernatant fraction. A higher level of deamidation was detected at the same Asn[309] residue (>15%), and deamidation at another Asn site, Asn[378] (>10%), was also identified in the total stressed sample and in the pellet fraction. In addition, very low levels of oxidation at Met[246] (~3%) and Met[422] (~1%) were also observed in the pellet fraction of the stressed sample.

For the thermally stressed mAb1 sample subjected to high temperature (90 °C), deamidation was observed for sixteen out of the total twenty-five Asn residues, including fourteen Asn sites that were unmodified under lower temperature stress conditions (65 °C/pH 8.5). The T_m of mAb1 in 10 mM sodium acetate, pH 5, is ~74.2 °C, which might provide an explanation for the differences in chemical modifications between the two samples stressed at different temperatures on either side of the T_m. High temperature has a direct effect on the conformation of quaternary, tertiary, and secondary structure and can lead to temperature-induced unfolding (8). This is consistent with the observations in our accompanying article (28) that the 90C stressed sample is the most extreme case of disruption of protein secondary and tertiary structure. Even the protein remaining in solution showed a significantly altered conformation. As a result, amino acid residues that are buried in the native form might be exposed to the solvent under this extreme thermal stress condition. It is also worth noting that eight Asn residues,

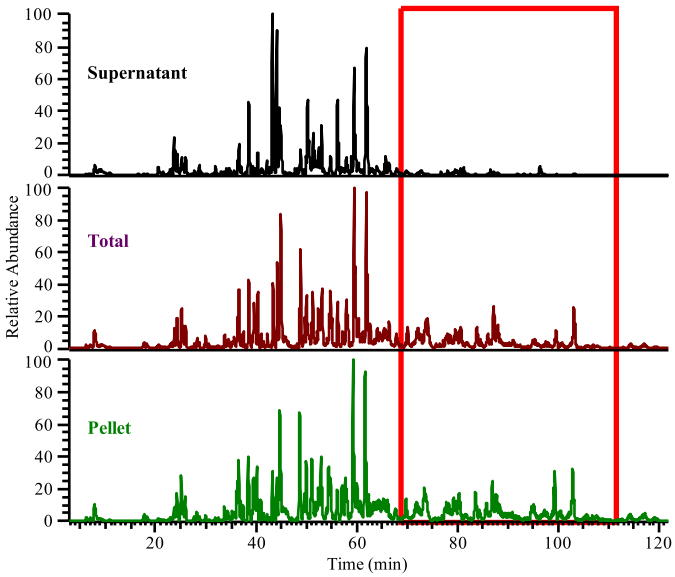

FIGURE 6. *Top panel,* trypsin peptide map of the supernatant fraction of the thermally stressed (90C) sample. *Middle panel,* trypsin peptide map of the total thermally stressed (90C) sample. *Bottom panel,* trypsin peptide map of the pellet fraction of the thermally stressed (90C) sample.

which showed high levels of deamidation (12.1–64.7%) in the total stressed sample and the pellet fraction of the 90C stressed sample, were not detected in the supernatant fraction (Table 4). Some peptides, which eluted late in the gradient, were not detected in the supernatant of the stressed sample (Fig. 6), indicating that peptide bond cleavage might occur under these extreme thermal conditions, and those peptides might be co-precipitated with the aggregates during the fractionation by centrifugation. The obtained results are consistent with a previous report showing that fragmentation occurred at elevated temperature for IgG_1 monoclonal antibodies (35).

Mapping of Chemical Modifications onto a Model Structure—To visualize the distribution of chemically modified residues within the mAb1 molecule, modified amino acids were mapped onto a three-dimensional antibody model structure. Because a full-length human IgG_2 experimentally derived structure is not yet available in the PDB (37), chemical modifications associated with the applied stresses were mapped onto the crystal structure of human antibody IgG_1 b12, PDB entry 1HZH (Fig. 7) (34). Amino acids modified under mechanical and chemical stress have similar patterns and are distributed over the entire molecule (Fig. 7, *A* and *C*). In contrast, the two His residues that were modified only in the metal-catalyzed oxidation sample, His^{304} and His^{427}, were in close proximity to Met^{246} in the Fc portion, which is the Met with the highest level of oxidation (>20%) (Fig. 7*D*). The preferential oxidation of His^{304}, His^{427}, and Met^{246} might be attributed to the formation of a putative copper-binding site on mAb1 in the vicinity of imidazole and thiol moieties (Fig. 7*D*). Because of the highest level of disruption of protein structure, thermal stress (90C), as expected, showed a larger area of the molecule had been modified; however, only deamidation, and no oxidation, was observed (Fig. 7*B*).

DISCUSSION

As demonstrated previously (8, 28), there are many different paths to protein aggregation, and the resulting aggregates can show very different characteristics. To investigate the role that chemical modifications might play in protein aggregation, mAb1 was stressed under various conditions to generate aggregates, including mechanical stress, chemical treatment, and thermal stress. The chemical modifications resulting from these stress conditions were then assessed. Table 5 shows the summary in biophysical and biochemical characteristics of the mAb1 aggregates generated under different conditions. The extent of unfolding of these different aggregate groups was assessed by FTIR in our accompanying article (28) and is shown in Table 5 for comparison purposes.

Previous work on assessing the immunogenicity of protein aggregates was done using copper treatment as the stress to generate those aggregates (38, 39). A unique feature observed during metal-catalyzed oxidation of proteins is that the amino acids near the metal-binding site are most susceptible to oxidation (26, 27). The amino acids that are common for the coordination of metals to proteins have been found to be His and Cys (40). His oxidation was observed in the metal-catalyzed aggregate analyzed here but was not seen with any other stresses. More importantly, our accompanying article (28) shows that a high level of copper was present in the metal-catalyzed samples determined by inductively coupled plasma mass spectrometry. A protein-free buffer treated identically to the test samples was used as a control to ensure that the metal ions were completely removed. The characterization of the copper-generated aggregates suggests that they are not representative of aggregates formed during normal process and storage conditions and therefore are not appropriate to use as representative of most protein aggregates in immunogenicity studies.

One mechanism for protein aggregate formation depends on conformational stability. Thermal stress typically results in aggregation via this process. The native protein first undergoes a reversible conformational change to an aggregation-prone state, which subsequently assembles irreversibly to the aggregated state (8). Other mechanisms of aggregation include colloidal stability, in which the interactions between the protein and the buffer result in decreased solubility or an increased propensity for self-association, and unfolding due to interactions at the air-liquid interface or other surfaces, usually mediated by hydrophobicity, and other surface interactions (41–43). Mechanical stress may cause denaturation and aggregation because of air-liquid interfaces, material surfaces, shear forces, cavitation, local thermal effects, etc. Rapid mass transfer of material to and from the air-liquid interface also occurs. Mixing of the aggregated or unfolded species from the surface into the bulk material can increase potential nucleation sites, although the mass transfer of previously nonexposed material to the interface results in the exposure of more protein to this potentially denaturing surface. Mechanical stress results in spontaneous adsorption of protein molecules to the enlarged air-liquid interface, which can result in the expansion and unfolding of the proteins, and thus trigger the formation of aggregates (43). The mixing of the protein with the air-liquid interface also

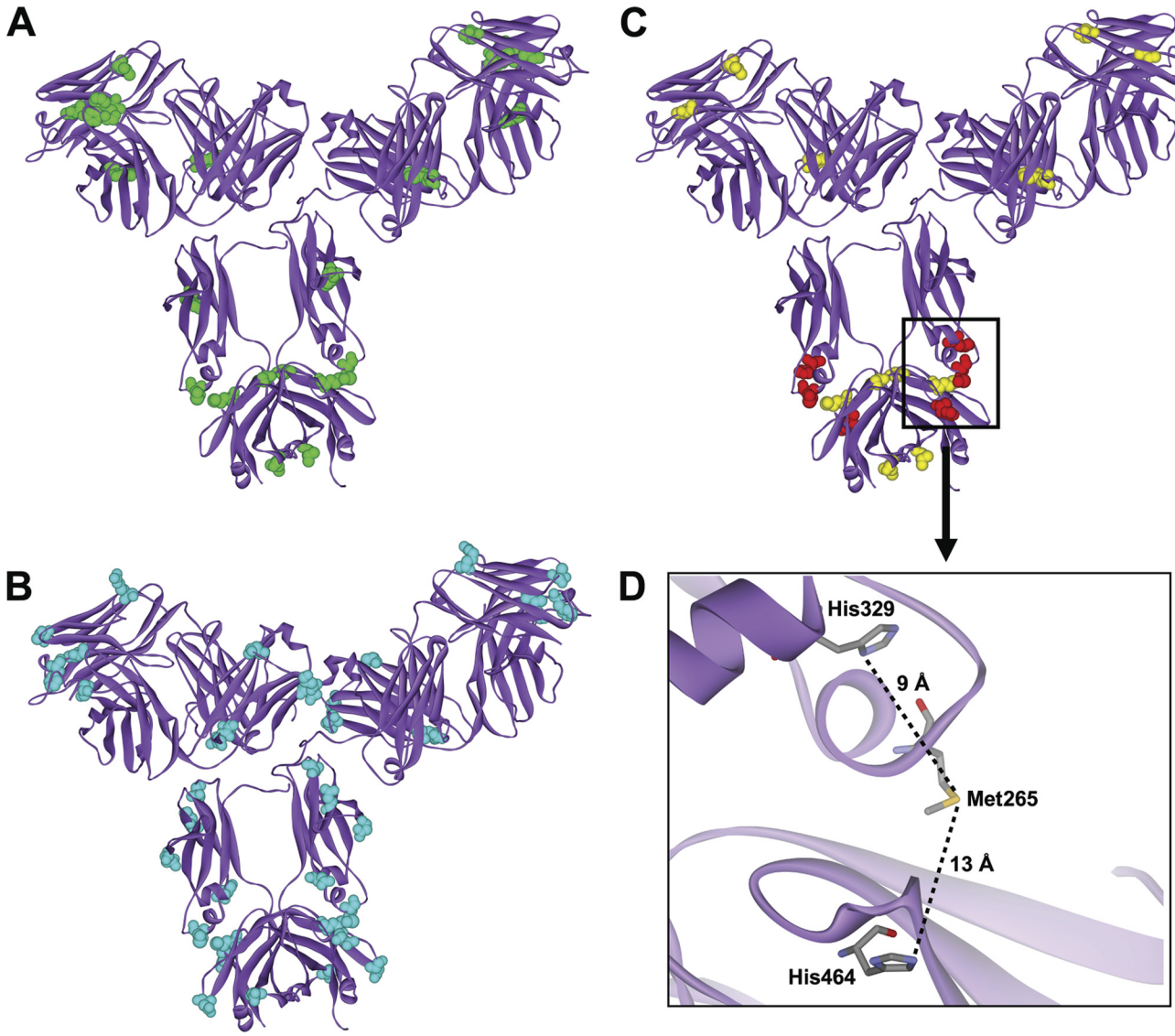

FIGURE 7. **Location of modified residues derived from stress studies of mAb1, displayed on the crystal structure of an IgG_1 molecule.** Modified mAb1 amino acids are colored by stress method at their corresponding positions in the antibody IgG_1 b12 crystal structure (PDB entry 1HZH). Residues are shown for mechanical stress (*green*) (*A*), thermal stress (*blue*) (*B*), and chemical treatment (*yellow*) (*C*), of which a potential copper-binding cluster is highlighted (*red*) (*D*), close up of a cluster of amino acids oxidized by metal-catalyzed oxidation. Residues of the IgG_1 crystal structure, Met^{265}, His^{329}, and His^{464}, correspond to oxidized mAb1 residues, Met^{246}, His^{304}, and His^{427}, respectively.

increases the exposure of the protein to air, which can lead to increased susceptibility to oxidation. The oxidation might in turn prevent the unfolded or partially unfolded protein from returning to the native structure and facilitate the aggregation. Met and/or Trp oxidations are the only chemical modifications identified in the mechanically stressed mAb1 samples. A higher level of Met oxidation was observed in the pellet fraction of the syringe-stressed samples than was seen in the total stressed samples and the supernatant fractions. As shown in our accompanying article (28), the total syringe-stressed sample and their supernatant fractions showed similar folded secondary structure. The susceptibility of a Met residue to oxidation is highly dependent on its solvent accessibility. Met^{246}, which is highly exposed to solvent, is the only oxidized Met residue observed in the supernatant fractions and total syringe-stressed samples. However, the secondary structure of protein in the pellet fractions showed some degree of perturbation, indicating that syringe-stressed aggregation might result in increased exposure of the protein to the air-liquid interface, oxygen, and subsequently increased susceptibility to oxidation. It is possible that aggregate formation occurs independently from oxidation, with the structural perturbation occurring at the interface and contributing to both phenomena. Alternatively, the oxidation could increase the aggregation propensity of the protein, or aggregate formation could lead to oxidation; more experiments are required to help clarify the order and dependence of the chemical modification and aggregate formation.

Stirring was found to be a very harsh condition to induce aggregation, with the extent of aggregation dependent on the duration of stress given to the system (43). As shown in Table 5, the protein in the stirred for 3 day sample was more unfolded than was seen in the sample generated by stirring for 20 h. Upon a progression of stirring from 20 h to 3 days, the level of Met and Trp oxidation increased, which is consistent with the increased

TABLE 5
Trend in biophysical and biochemical characteristics of the mAb1 aggregates stressed under different conditions

Stress treatment[a]	Folded secondary structure[b] (super./pellet)	Chemical modification[c]			
		Met (O)	Trp (O)	His (O)	Asn (D)
Untreated	Fold./- -[d]	–[e]	–	–	–
Metal	Fold./Unfold.	Site-specific, partial[f]	Site-specific, partial	Site-specific, partial	–
H_2O_2	Fold./- -[d]	Solvent-exposed, complete[g]	–	–	–
Syringe-so$^-$	Fold./- -[d]	Some, partial[h]	–	–	–
Syringe-so$^+$	Fold./Int.	Some, partial	–	–	–
Stir-20h	Fold./Int.	All, partial[h]	Few, partial[h]	–	–
Stir-3d	Fold./Unfold.	All, partial	Some, partial	–	–
65C/pH 8.5	Fold./Unfold.	–	–	–	Solvent-exposed, partial[g]
90C	Int./Unfold.	–	–	–	Many, extensive[i]

[a] For detailed stress conditions see our accompanying article (28).
[b] In our accompanying article (28), the folded secondary structure was assessed by FTIR by comparing the spectra of the supernatant (super.)/pellet (pellet) fractions with the untreated sample. Spectral similarity is shown here as folded (Fold.) (≥89%), intermediate (Int.) (30–88%), or unfolded (Unfold.) (≤29%).
[c] Met oxidation, Trp oxidation, His oxidation, and Asn deamidation are shown.
[d] - - means not tested.
[e] – means not detected.
[f] Site-specific amino acid residues were partially modified.
[g] Solvent-exposed amino acid residues were complete/partially modified.
[h] Few, some, and all amino acid residues were partially modified.
[i] Many amino acid residues were extensively modified.

exposure to the surface that would occur with a longer duration of stirring. In addition to an enlarged air-liquid interface, stirring stress also results in rapid transportation of denaturated, aggregated, or modified species into solution because of the turbulent flow (8), which might provide an explanation for the similar level of oxidation in the supernatant and pellet fractions of the stirring stressed samples. The adsorbed/oxidized species was rapidly transported into solution, thus facilitating further aggregation within the bulk. As a result, the oxidized protein was present at similar levels in the pellet and supernatant fractions after rigorous and long time stirring. In contrast, under the syringe stress condition, the protein adsorbed at the air-liquid interface and then aggregated, and the modified or aggregated species were not transported back into solution as efficiently as under the conditions of stirring stress. In addition, the levels of oxidation in different stirred samples (pellet *versus* supernatant) showed no significant difference, which suggests that oxidation is not the key factor in aggregation of the pelleted material. As further support, addition of the antioxidant methionine did not help to prevent aggregation in the stirring stressed samples (data not shown), which agrees with the assumption that oxidation is not the key factor in aggregation. However, further in-depth studies still need to be conducted to confirm this observation.

Several studies on Met oxidation in monoclonal antibodies exposed to oxidant have been reported (16, 44). Susceptibility of Met residues to oxidation is highly dependent on their solvent exposure and location in the three-dimensional structure of the antibody. The Met residues in the Fc portion are more exposed to solvent than other Met residues in the Fab portion, which might provide an explanation for the higher levels of oxidation of Met residues in the Fc portion after treatment with H_2O_2. The chemical modifications (Met oxidation) seen with mild stirring are similar to those seen with H_2O_2 treatment, which suggests that mild stirring stress increases interactions of the protein with air, most likely by increasing contact at the renewed air-liquid interface as described in a previous report (43). Lerner and co-workers (45) and Liu *et al.* (46) reported that antibodies can convert molecular oxygen into hydrogen peroxide, which might provide an additional explanation for the similar pattern of Met oxidation in the mild stirring stressed and H_2O_2-treated samples. The fact that oxidation occurs in the same regions of the molecule, which are highly surface-accessible, under mild stirring stress and H_2O_2 treatment suggests that there is no significant unfolding of the protein or exposure of regions that are primarily protected in the native state. In contrast, stirring for 3 days results in more modification with more unfolded structure and more exposure of hydrophobic regions normally in the interior of the protein.

Elevated temperature and prolonged incubation time have been shown to increase the amount of aggregates of monoclonal antibodies (8, 44, 47). An increase in temperature accelerates both chemical modifications of the proteins and the amount of aggregate formed. Higher temperature also has a direct effect on the level of quaternary, tertiary, and secondary structure of a protein and in general reflects the conformational stability of a protein and can lead to temperature-induced unfolding. The aggregates generated by thermal stress showed significant deamidation but almost no oxidation. This is consistent with the hypothesis that high temperature-induced aggregation involves primarily conformational stability. The protein unfolds, exposing regions that are normally protected, which then immediately aggregate to decrease surface exposure of these hydrophobic residues. Previous reports (48) have shown that secondary structure formation prevents Asn from deamidation due to restrained flexibility of local structure, which might provide an explanation for the low levels of deamidation observed only at solvent-exposed Asn residues in the 65C/pH 8.5 stressed sample. In contrast, many Asn residues are extensively deamidated in the 90C stressed sample because of the most extreme disruption of protein secondary and tertiary structures. The lack of oxidation is also consistent with the lack of exposure to the air-liquid interface during thermal stress.

We cannot conclude from these results whether the modifications occurred after aggregation or if the modifications reported here occurred first and are contributing factors to aggregation. But having identified which modifications can occur during various conditions will now allow us to begin

addressing these mechanistic questions. Furthermore, the exact type, location, and level of chemical modification can serve as a diagnostic tool to infer the stress conditions leading to aggregation.

Acknowledgments—We thank Izydor Apostol and Drew Kelner for their support and technical discussion.

REFERENCES

1. Brekke, O. H., and Sandlie, I. (2003) *Nat. Rev. Drug Discov.* **2,** 52–62
2. Schrama, D., Reisfeld, R. A., and Becker, J. C. (2006) *Nat. Rev. Drug Discov.* **5,** 147–159
3. Bebbington, C., and Yarranton, G. (2008) *Curr. Opin. Biotechnol.* **19,** 613–619
4. Braun, A., Kwee, L., Labow, M. A., and Alsenz, J. (1997) *Pharm. Res.* **14,** 1472–1478
5. Bucciantini, M., Giannoni, E., Chiti, F., Baroni, F., Formigli, L., Zurdo, J., Taddei, N., Ramponi, G., Dobson, C. M., and Stefani, M. (2002) *Nature* **416,** 507–511
6. Demeule, B., Gurny, R., and Arvinte, T. (2006) *Eur. J. Pharm. Biopharm.* **62,** 121–130
7. Ryan, M. E., Webster, M. L., and Statler, J. D. (1996) *Clin. Pediatr.* **35,** 23–31
8. Mahler, H. C., Friess, W., Grauschopf, U., and Kiese, S. (2009) *J. Pharm. Sci.* **98,** 2909–2934
9. Zhang, Z., Pan, H., and Chen, X. (2009) *Mass Spectrom. Rev.* **28,** 147–176
10. Huang, L., Lu, J., Wroblewski, V. J., Beals, J. M., and Riggin, R. M. (2005) *Anal. Chem.* **77,** 1432–1439
11. Robinson, N. E., and Robinson, A. B. (2001) *Proc. Natl. Acad. Sci. U.S.A.* **98,** 12409–12413
12. Kosky, A. A., Razzaq, U. O., Treuheit, M. J., and Brems, D. N. (1999) *Protein Sci.* **8,** 2519–2523
13. Geiger, T., and Clarke, S. (1987) *J. Biol. Chem.* **262,** 785–794
14. Liu, Y. D., van Enk, J. Z., and Flynn, G. C. (2009) *Biologicals* **37,** 313–322
15. Men, L., and Wang, Y. (2007) *J. Proteome Res.* **6,** 216–225
16. Pan, H., Chen, K., Chu, L., Kinderman, F., Apostol, I., and Huang, G. (2009) *Protein Sci.* **18,** 424–433
17. Finley, E. L., Dillon, J., Crouch, R. K., and Schey, K. L. (1998) *Protein Sci.* **7,** 2391–2397
18. Schöneich, C. (2000) *J. Pharm. Biomed. Anal.* **21,** 1093–1097
19. Ji, J. A., Zhang, B., Cheng, W., and Wang, Y. J. (2009) *J. Pharm. Sci.* **98,** 4485–4500
20. Bee, J. S., Nelson, S. A., Freund, E., Carpenter, J. F., and Randolph, T. W. (2009) *J. Pharm. Sci.* **98,** 3290–3301
21. Jiang, Y., Nashed-Samuel, Y., Li, C., Liu, W., Pollastrini, J., Mallard, D., Wen, Z. Q., Fujimori, K., Pallitto, M., Donahue, L., Chu, G., Torraca, G., Vance, A., Mire-Sluis, T., Freund, E., Davis, J., and Narhi, L. O. (2009) *J. Pharm. Sci.* **98,** 4695–4710
22. Lam, X. M., Yang, J. Y., and Cleland, J. L. (1997) *J. Pharm. Sci.* **86,** 1250–1255
23. Kerwin, B. A. (2008) *J. Pharm. Sci.* **97,** 2924–2935
24. Hlavaty, J. J., and Nowak, T. (1997) *Biochemistry* **36,** 15514–15525
25. Lim, J., and Vachet, R. W. (2003) *Anal. Chem.* **75,** 1164–1172
26. Li, S., Nguyen, T. H., Schöneich, C., and Borchardt, R. T. (1995) *Biochemistry* **34,** 5762–5772
27. Zhao, F., Ghezzo-Schöneich, E., Aced, G. I., Hong, J., Milby, T., and Schöneich, C. (1997) *J. Biol. Chem.* **272,** 9019–9029
28. Joubert, M. K., Luo, Q., Nashed-Samuel, Y., Wypych, J., and Narhi, L. O. (2011) *J. Biol. Chem.* **286,** 25118–25133
29. Shukla, A. A., Hubbard, B., Tressel, T., Guhan, S., and Low, D. J. (2007) *J. Chromatogr. B Analyt Technol. Biomed. Life Sci.* **848,** 28–39
30. Zhang, Z. (2004) *Anal. Chem.* **76,** 6374–6383
31. Halgren, T. A. (1996) *J. Comp. Chem.* **17,** 490–519
32. Ramachandran, G. N., Ramakrishnan, C., and Sasisekharan, V. (1963) *J. Mol. Biol.* **7,** 95–99
33. Cruickshank, D. W. (1959) in *International Tables for X-ray Crystallography* (Kasper, J. S. and Lonsdale, K., eds) Vol. 2, pp. 331–332, Kynoch Press, Birmingham, AL
34. Saphire, E. O., Parren, P. W., Pantophlet, R., Zwick, M. B., Morris, G. M., Rudd, P. M., Dwek, R. A., Stanfield, R. L., Burton, D. R., and Wilson, I. A. (2001) *Science* **293,** 1155–1159
35. Liu, H., Gaza-Bulseco, G., and Sun, J. (2006) *J. Chromatogr. B Analyt. Technol. Biomed. Life Sci.* **837,** 35–43
36. Maria, C. S., Revilla, E., Ayala, A., de la Cruz, C. P., and Machado, A. (1995) *FEBS Lett.* **374,** 85–88
37. Berman, H., Henrick, K., and Nakamura, H. (2003) *Nat. Struct. Biol.* **10,** 980
38. Hermeling, S., Schellekens, H., Maas, C., Gebbink, M. F., Crommelin, D. J., and Jiskoot, W. (2006) *J. Pharm. Sci.* **95,** 1084–1096
39. Ba°alp, A., Mustafaeva, Z., and Mustafaev, M. (2002) *Hybrid Hybridomics* **21,** 45–51
40. Ueda, E. K., Gout, P. W., and Morganti, L. (2003) *J. Chromatogr. A* **988,** 1–23
41. Mahler, H. C., Müller, R., Friess, W., Delille, A., and Matheus, S. (2005) *Eur. J. Pharm. Biopharm.* **59,** 407–417
42. Chi, E. Y., Krishnan, S., Kendrick, B. S., Chang, B. S., Carpenter, J. F., and Randolph, T. W. (2003) *Protein Sci.* **12,** 903–913
43. Kiese, S., Papppenberger, A., Friess, W., and Mahler, H. C. (2008) *J. Pharm. Sci.* **97,** 4347–4366
44. Chumsae, C., Gaza-Bulseco, G., Sun, J., and Liu, H. (2007) *J. Chromatogr. B* **850,** 285–294
45. Wentworth, A. D., Jones, L. H., Wentworth, P., Jr., Janda, K. D., and Lerner, R. A. (2000) *Proc. Natl. Acad. Sci. U.S.A.* **97,** 10930–10935
46. Wentworth, P., Jr., Jones, L. H., Wentworth, A. D., Zhu, X., Larsen, N. A., Wilson, I. A., Xu, X., Goddard, W. A., 3rd, Janda, K. D., Eschenmoser, A., and Lerner, R. A. (2001) *Science* **293,** 1806–1811
47. Liu, H., Gaza-Bulseco, G., Faldu, D., Chumsae, C., and Sun, J. (2008) *J. Pharm. Sci.* **97,** 2426–2447
48. Nonaka, Y., Aizawa, T., Akieda, D., Yasui, M., Watanabe, M., Watanabe, N., Tanaka, I., Kamiya, M., Mizuguchi, M., Demura, M., and Kawano, K. (2008) *Proteins* **72,** 313–322